

A Low-Complexity, Low-Cycle-Slip-Probability, Format-Independent Carrier Estimator with Adaptive Filter Length

Adaickalavan Meiyappan, *Student Member, IEEE*, Hoon Kim, *Senior Member, IEEE*, and Pooi-Yuen Kam, *Fellow, IEEE*

Abstract—We present a low-complexity carrier estimator with an effective filter length that automatically adapts according to the signal-to-noise ratio, laser-linewidth-symbol-duration product, nonlinear phase noise, and modulation format. Laser-linewidth and frequency-offset tolerances are studied. The filter length of a carrier estimator is shown to affect the cycle slip probability besides the bit-error rate (BER) performance. Considering that forward-error-correction codes are not robust to burst errors and phase slips, we demonstrate that filter-length optimization is necessary to avoid spectral-efficiency reduction in pilot assisted systems and potential system failures in differential encoding systems. Our estimator achieves a lower cycle slip probability and a greater nonlinear phase noise tolerance than DiffFE-MPE, DiffFE-BPS, and complex-weighted decision-aided maximum-likelihood (CW-DA-ML) estimator. DiffFE-MPE and DiffFE-BPS refer to the differential frequency estimator (DiffFE) followed by block M th power phase estimator (MPE) and blind phase search (BPS), respectively. For a 4100 km quaternary phase-shift keying transmission at a BER of 2.5×10^{-2} , our estimator achieves a cycle slip probability of 2.9×10^{-7} compared to 5.6×10^{-6} , 5.3×10^{-6} , and 3.2×10^{-7} for DiffFE-MPE, DiffFE-BPS, and CW-DA-ML, respectively.

Index Terms—Blind phase search, block M th power, forward error correction, frequency offset, nonlinear optics, phase noise.

I. INTRODUCTION

EARLY optical networking systems provided point-to-point wavelength-division multiplexed (WDM) transmission. The WDM channels propagated over predetermined optical path between fixed transmitter-receiver pairs, with preset symbol rate and modulation format. These point-to-point systems then evolved into optical mesh topologies using WDM and reconfigurable optical add/drop multiplexers, developed to minimize optical-electrical-optical wavelength regeneration and grooming costs at intermediate nodes [1]. Later, optical packet switching (OPS) offering sub-wavelength switching granularity emerged, driven by the desire for rapidly reconfigurable circuits

and effective accommodation of bursty traffic [2]. Unlike early WDM systems, packets can be dynamically routed over different optical paths depending on link status (e.g., link availability and delay), thus experiencing different link impairments. Moreover, with no fixed transmitter-receiver pairs, a given receiver may receive packets from different transmitters. Currently, elastic optical networks [3] and software defined networks [4] have been touted as solutions for enhanced spectral efficiency and optimized network resource utilization. These architectures require transceivers with tunable modulation format and symbol rate to support tradeoffs among optical reach, bit rate, and spectral occupancy [5]. A continuous tradeoff between optical reach and spectral efficiency was demonstrated by time-domain interleaving of different M -ary phase-shift keying (MPSK) and M -ary quadrature amplitude modulation (MQAM) signals [6], [7]. Recently, flexible modulation format and bit rate depending on light-path length was shown to reduce queuing delay in OPS networks [8].

Considering the above progress towards a fully reconfigurable optical network, the carrier estimators in intradyne coherent receivers are expected to receive dynamic data with different signal-to-noise ratios (SNRs) and nonlinear phase noise due to variable link impairments, different laser phase noise and frequency offsets due to variable transmitter-receiver laser pairs, different modulation formats, and different symbol rates. The popular phase estimators, namely, block M th power phase estimator (MPE) [9] and blind phase search (BPS) [10], utilize fixed-length transversal filters. Their optimum filter length with respect to bit-error rate (BER) depends on the parameter set of SNR, laser-linewidth-symbol-duration product $\Delta\nu T$, nonlinear phase noise, and modulation format [10]–[12]. Difficult numerical optimization and manual adjustment of filter length are needed for each set of parameters [10]–[12], which may not be practical in a reconfigurable optical network. Note that the computational complexity of BPS increases with its filter length. The popular frequency estimator, namely, differential frequency estimator (DiffFE) [13] offers a limited frequency-offset-symbol-duration product $\Delta f T$ estimation range of $\pm 1/2M$ for MPSK signals. Furthermore, MPE and DiffFE are not format transparent. In order to support multiple formats, several format-adapted MPE modules and format-adapted DiffFE modules are required, thus increasing the receiver hardware.

Previously, we had derived a decision-aided maximum-likelihood (DA-ML) phase estimator using a fixed-length filter in [14]. A first-order recursion technique was proposed in [15] to

Manuscript received August 7, 2013; revised September 20, 2013; accepted September 28, 2013. Date of publication October 8, 2013; date of current version November 18, 2013. This work was supported by the Singapore MoE under AcRF Tier 2 Grant MOE2010-T2-1-101.

The authors are with the Department of Electrical and Computer Engineering, National University of Singapore, 117576 Singapore (e-mail: adaickalavan@hotmail.com; hoonkim@ieee.org; elekampy@nus.edu.sg).

Color versions of one or more of the figures in this paper are available online at <http://ieeexplore.ieee.org>.

Digital Object Identifier 10.1109/JLT.2013.2285155

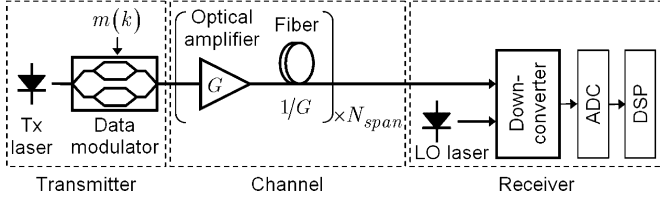


Fig. 1. Optical transmission system employing inline amplifiers. ADC: analog-to-digital converter, DSP: digital signal processor, Tx: transmitter.

avoid the fixed-length filter of DA-ML. However, the phase estimators of [14] and [15], which employ real filter weights, have a severely limited ΔfT tolerance in the range of 10^{-3} [16]. Hence, by replacing the filter weights of DA-ML with complex weights, a complex-weighted DA-ML (CW-DA-ML) joint phase and frequency estimator was presented in [17]. Recently, to avoid the manual filter-length optimization of CW-DA-ML, we developed an adaptive CW-DA estimator with an adaptive filter length [18] following the idea in [15].

In this paper, the $\Delta\nu T$ tolerance, nonlinear phase noise tolerance, and cycle slip probability in linear and nonlinear phase noise scenarios are investigated via simulation for the adaptive CW-DA estimator. Furthermore, we show that filter-length optimization is crucial since it affects the cycle slip probability besides the BER performance. Performance measures of adaptive CW-DA estimator are benchmarked against DiffFE-MPE, DiffFE-BPS, and CW-DA-ML. DiffFE-MPE and DiffFE-BPS refer to the operation of DiffFE followed by MPE and BPS, respectively. In BPS, we set the number of test phases β to 32 following [10].

The organization of this paper is as follows. In Section II, adaptive CW-DA estimator is derived and the adaptation of its effective filter length is explained. In Section III, the $\Delta\nu T$ tolerance, ΔfT tolerance, and cycle slip probability in the linear regime are investigated. In Section IV, the nonlinear phase noise tolerance and cycle slip probability in the nonlinear regime are studied. In Section V, a complexity analysis of the carrier estimators is performed. Section VI concludes the paper. Throughout this paper, $E[\cdot]$, superscript $*$, and superscript T , denotes the expectation operator, complex conjugate, and transpose, respectively.

II. ADAPTIVE CW-DA ESTIMATOR

A. System Model

Consider the canonical coherent optical transmission system shown in Fig. 1. At the transmitter, the k th symbol $m(k)$ is up-converted from electrical to optical signal and transmitted into an optical channel. The channel employs N_{span} zero-dispersion fiber spans of equal length L_{fiber} . Fiber loss in each span is compensated exactly by an inline erbium-doped fiber amplifier (EDFA) of gain $G = \exp(\alpha L_{fiber})$ where α is the attenuation coefficient. At the output of the i th EDFA, amplified spontaneous emission (ASE) noise n_i is added to the signal. Noise n_i is zero-mean circularly symmetric complex Gaussian with spectral density of $S_{sp} = (G - 1)h\nu n_{sp}$, where $h\nu$ is the photon energy and n_{sp} is the spontaneous-emission factor. At the

receiver, optical-to-electrical downconversion is performed in an intradyne coherent receiver by mixing with a local oscillator (LO) laser followed by balanced photodetection. The k th received sample arriving at the carrier estimator is modeled as

$$r(k) = m(k)e^{j(\theta(k) + \Delta\omega k)} + n(k), \quad k = 0, 1, 2, \dots \quad (1)$$

Here, $\theta(k)$ represents the phase noise impairment in the received sample. We have $\theta(k) = \theta_L(k)$ in the linear regime, where $\theta_L(k)$ is the laser phase noise modeled as a Wiener process. The laser phase-noise increment $\theta_L(k) - \theta_L(k-1)$ has mean zero and variance $\sigma_p^2 = 2\pi\Delta\nu T$, where $\Delta\nu$ is the combined laser linewidth of the transmitter and LO lasers. The angular frequency offset between the transmitter and LO lasers is denoted as $\Delta\omega = 2\pi\Delta fT$. In (1), $n(k)$ represents the accumulated ASE noise with mean zero and variance $N_0 = N_{span}S_{sp}B_0$, where B_0 is a filter bandwidth matched to the signal. The SNR per bit is defined as $\gamma_b = E[|m(k)|^2]/N_0 \log_2 M$. In order to be robust against cycle slips in the carrier estimator, differential encoding of data is assumed.

B. Adaptive CW-DA Algorithm

In CW-DA-ML [17], the carrier at time $k+1$ is estimated by a complex phasor $V(k+1)$. The sample $r(k+1)$ is corrected by derotating it as $r(k+1)V^*(k+1)$. The phasor $V(k+1)$ is formed using a transversal filter of length L as

$$V(k+1) = C(k) \sum_{l=k-L+1}^k w_{k+1-l}(k)r(l)\hat{m}^*(l) \quad (2)$$

where $C^{-1}(k) = \sum_{l=k-L+1}^k |\hat{m}(l)|^2$ is a normalizing factor, $w_i(k)$ is the i th complex filter weight, and $\hat{m}(l)$ is the symbol decision on $r(l)V^*(l)$ made using a minimum Euclidean-distance metric.

To avoid specifying a filter length L , we propose to replace (2) with a new complex phasor $\bar{V}(k+1)$ formed by a first-order recursion as

$$\bar{V}(k+1) = \bar{w}_1\bar{V}(k) + \bar{w}_2x(k) \quad (3)$$

where \bar{w}_i is the new i th complex filter weight and $x(k)$ is the normalized filter input $r(k)/\hat{m}(k)$. If $\hat{m}(k) = m(k)$, $x(k)$ approximates the carrier at time k . Using $x(k)$ as the desired response, we define the estimation error as the difference between $x(k)$ and $\bar{V}(k)$. The filter weights in (3) are recomputed automatically at each time $k \geq 1$ so as to minimize the sum-of-error-squares cost function $J(k)$, where

$$J(k) = \sum_{l=1}^k |x(l) - \bar{V}(l)|^2. \quad (4)$$

In (4), $\bar{V}(l)$ is expressed in terms of (3). At time $k=0$, we initialize $\bar{V}(0) = 1$, $\bar{w}_1 = 0$, and $\bar{w}_2 = 1$. Solving $\partial J(k)/\partial \bar{w}^* = 0$, where $\bar{w} = [\bar{w}_1 \ \bar{w}_2]^T$, yields the least-squares optimum \bar{w} at

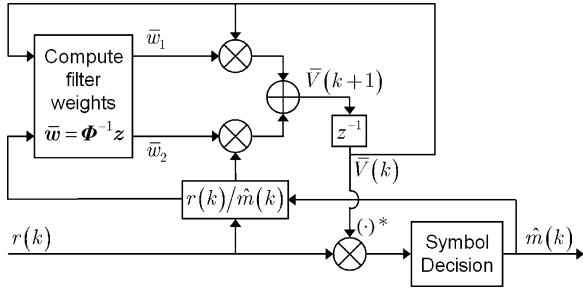
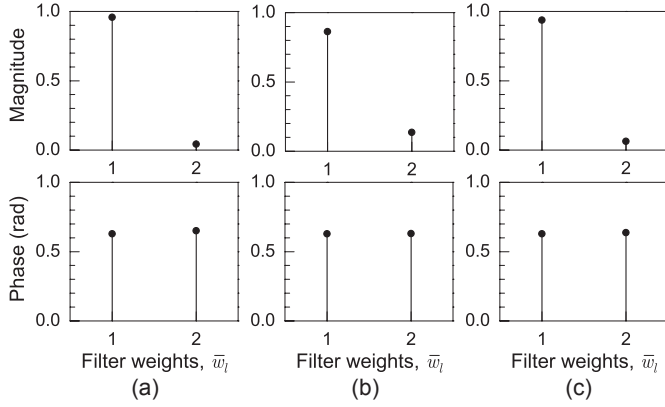


Fig. 2. Adaptive CW-DA estimator.

Fig. 3. Steady-state filter weights at (a) $\gamma_b = 12$ dB with $\Delta\nu T = 10^{-6}$, (b) $\gamma_b = 12$ dB with $\Delta\nu T = 10^{-4}$, and (c) $\gamma_b = 4$ dB with $\Delta\nu T = 10^{-4}$. Here, $\Delta f T = 0.1$.

time k as

$$\bar{\mathbf{w}} = \Phi^{-1} \mathbf{z} \quad (5)$$

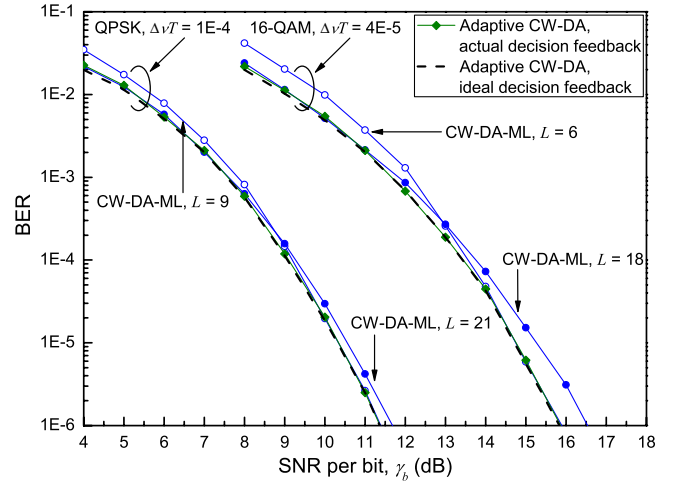
$$\Phi = \sum_{l=1}^k \begin{bmatrix} |\bar{V}(l-1)|^2 & \bar{V}^*(l-1)x(l-1) \\ x^*(l-1)\bar{V}(l-1) & |x(l-1)|^2 \end{bmatrix} \quad (6)$$

$$\mathbf{z} = \sum_{l=1}^k x(l) \cdot \begin{bmatrix} \bar{V}^*(l-1) \\ x^*(l-1) \end{bmatrix} \quad (7)$$

where Φ is a 2-by-2 matrix and \mathbf{z} is a 2-by-1 vector. The structure of adaptive CW-DA estimator is shown in Fig. 2.

C. Adaptation of Effective Filter Length

The steady-state filter weights, averaged over 500 runs, of adaptive CW-DA estimator for quaternary PSK (QPSK) signals are plotted in Fig. 3. Magnitude of $\bar{V}(l)$ must approximate 1 to minimize the sum of error squares in (4) since the magnitude of $x(l)$ is ~ 1 . For this condition to be satisfied, the magnitude sum of the filter weights must equal 1 by virtue of (3). Indeed, $|\bar{w}_1| + |\bar{w}_2|$ always equal to ~ 1 in Fig. 3. Given the recursive nature of (3) and the sum $|\bar{w}_1| + |\bar{w}_2| \cong 1$, the filter input samples $\{x(l)\}$ will be summed in a decaying manner by (3). Thus, $|\bar{w}_1|$ is a measure of the effective filter length of our recursive filter. The effective filter length represented by $|\bar{w}_1|$ decreases from Fig. 3(a) to Fig. 3(b) and increases from Fig. 3(b) to Fig. 3(c) corresponding to the increase in $\Delta\nu T$ and decrease in SNR, respectively.

Fig. 4. BER performance. Here, $\Delta f T = 0.1$.

The phasor $\bar{V}(l)$ must have an angular frequency offset approximating $\Delta\omega l$ to minimize (4) since angular frequency offset of $x(l)$ is $\sim \Delta\omega l$. For this condition to be satisfied, the phase of \bar{w}_1 and \bar{w}_2 should be $\sim \Delta\omega$ by virtue of (3). Indeed, the phase of \bar{w}_1 and \bar{w}_2 always converge to the actual $\Delta\omega$ value of 0.2π rad in Fig. 3 regardless of SNR and $\Delta\nu T$.

Fig. 4 shows the BER performance of CW-DA-ML for QPSK and 16-QAM signals. The value $(LT)^{-1}$ is a measure of an estimator's bandwidth. The optimum value of L found by an exhaustive search is larger at low SNR and smaller at high SNR. Narrower bandwidth is beneficial at lower SNR to filter the dominant ASE noise and wider bandwidth is beneficial at higher SNR to track the dominant laser phase noise. On the flip side, adaptive CW-DA estimator always minimizes the BER by automatically adapting its effective filter length according to the SNR, $\Delta\nu T$, and modulation format. Performance loss of actual, compared to ideal, decision feedback is minimal for the tested SNR range.

III. PERFORMANCE IN LINEAR PHASE NOISE

Fig. 5 compares the laser linewidth and frequency offset tolerance of carrier estimators at a BER of 10^{-3} for QPSK signals. The γ_b penalty is referenced to that of ideal coherent detection. The filter length L in MPE, BPS, and CW-DA-ML is set to 15, 19, and 15, respectively, which are numerically optimized for a 1-dB γ_b penalty at BER of 10^{-3} [17]. For a 1-dB penalty, adaptive CW-DA estimator accommodates a $\Delta\nu T$ of 1.8×10^{-4} which is comparable to that of MPE and CW-DA-ML, but slightly smaller than the 4.1×10^{-4} $\Delta\nu T$ tolerance of BPS. As for the $\Delta f T$ estimation range, DiffFE is limited to $\pm 1/8$ due to the raising of samples to the 4th power for modulation removal. However, adaptive CW-DA estimator attains a complete $\Delta f T$ estimation range of $\pm 1/2$, as the phasor $V(k)$ has an unambiguous phase tracking range of $[0, 2\pi)$.

For an error-free optical communication, the optical reach without regeneration is limited by SNR. Forward error correction (FEC) is now widely adopted as a standard technique for increasing the optical reach or lowering the SNR

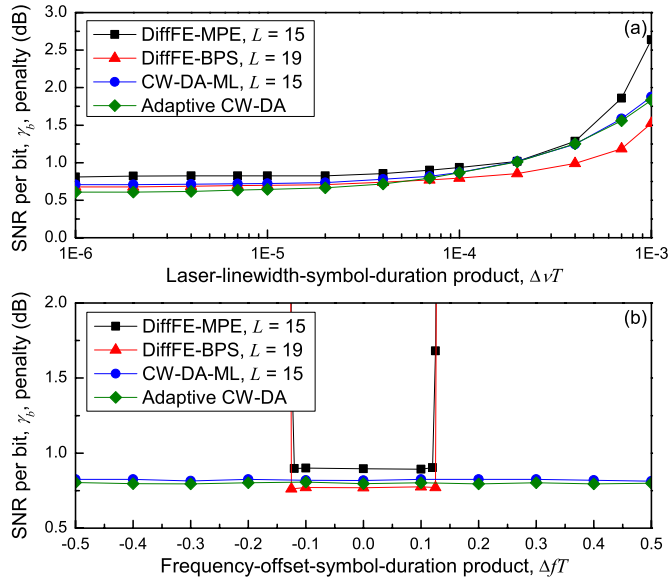


Fig. 5. (a) Laser linewidth tolerance, with $\Delta f T = 0.1$. (b) Frequency offset tolerance, with $\Delta\nu T = 7 \times 10^{-5}$.

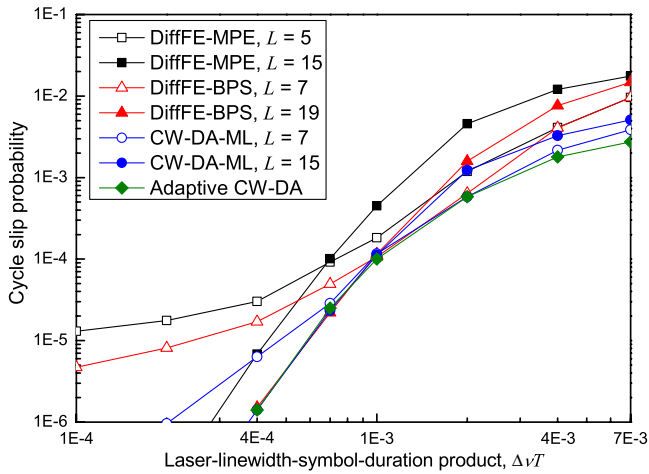


Fig. 6. Cycle slip probability of carrier estimators. Here, $\gamma_b = 7.82$ dB.

requirement [19]. In general, FEC codes are not designed for burst errors and correlated errors, which if encountered can tighten the BER threshold of the code [20].

Cycle slips are inherent in MPE, BPS, CW-DA-ML, and adaptive CW-DA estimator. Pilot symbols can be used to mitigate cycle slips, but errors due to cycle slips will persist until the next pilot symbols arrive resulting in burst errors. For successful FEC decoding, pilot symbols need to be inserted at a much higher frequency than the cycle slip probability to minimize the burst error length. Therefore, a low cycle slip probability is preferred to minimize the pilot overhead. The cycle slip probability is plotted in Fig. 6 using QPSK signals at $\gamma_b = 7.82$ dB. Cycle slip probability is seen to be filter-length dependent in DiffFE-MPE, DiffFE-BPS, and CW-DA-ML. Effective tracking of laser phase noise using shorter filter lengths at broader laser linewidths and sufficient averaging of ASE noise at narrower laser linewidths using longer filter lengths improves the phase

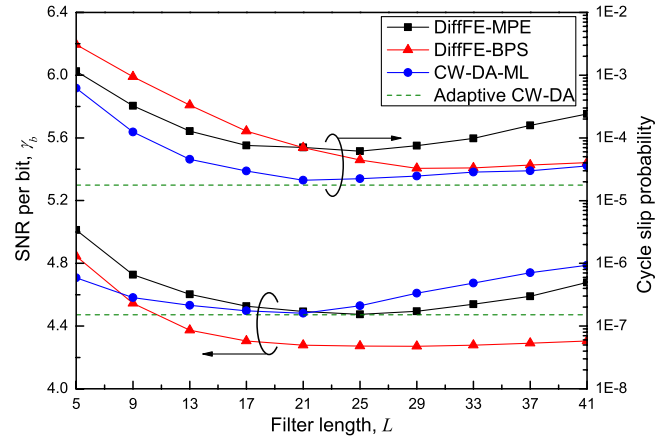


Fig. 7. Required SNR and corresponding cycle slip probability at a BER of 2.5×10^{-2} . Here, $\Delta\nu T = 3 \times 10^{-4}$.

estimate. Improved phase estimate reduces the cycle slip probability by reducing phase unwrapping errors in MPE and BPS, and by reducing the symbol decision errors in CW-DA-ML. Inappropriate selection of filter length can be detrimental. For example, insufficient filter length causes a cycle slip probability floor at smaller values of $\Delta\nu T$. Our adaptive CW-DA estimator tolerates a larger or equal $\Delta\nu T$ compared to DiffFE-MPE, DiffFE-BPS, and CW-DA-ML for a given cycle slip probability.

Next, we demonstrate the criticality of filter-length optimization in a differentially encoded system employing soft decision (SD) FEC. Instead of pilot symbols, differential encoding can be used to confine the catastrophic errors of a cycle slip to the slip duration. SD FEC provides enhanced net coding gain but its benefits are impaired by the error duplication penalty in differentially encoded systems [21]. The differential encoding penalty was shown to be completely eliminated by turbo differential decoding (TDD), i.e., turbo decoding of an outer SD low density parity check decoder and an inner soft differential decoder [21], [22]. However, TDD is vulnerable to a quickly rising post-FEC error floor in the presence of frequent cycle slips [22].

Fig. 7 plots the required SNR for QPSK signals with a target BER of 2.5×10^{-2} and the corresponding cycle slip probability as a function of the filter length. The cycle slip probability is more sensitive than the required SNR to variations in the filter length. For example, DiffFE-BPS attains a 0.58-dB improvement in the required SNR with filter-length optimization but achieves a 94 times reduction in cycle slip probability. Misadjustment of filter length L in DiffFE-MPE by 4 taps from 17 to 13 causes the cycle slip probability to rise above 10^{-4} , which would cause the TDD post-FEC BER to saturate above 10^{-9} [22]. Such misadjustments can render the carrier estimator unusable as high data integrity with BER lower than 10^{-9} , preferably 10^{-12} , is generally expected in optical transport systems. On the other hand, adaptive CW-DA estimator assures the lowest cycle slip probability at 1.8×10^{-5} and a TDD post-FEC BER of much lower than 10^{-9} . Simultaneously, our new estimator achieves a comparable SNR requirement to that of DiffFE-MPE and CW-DA-ML, and is a mere 0.2 dB inferior to DiffFE-BPS with optimum filter length.

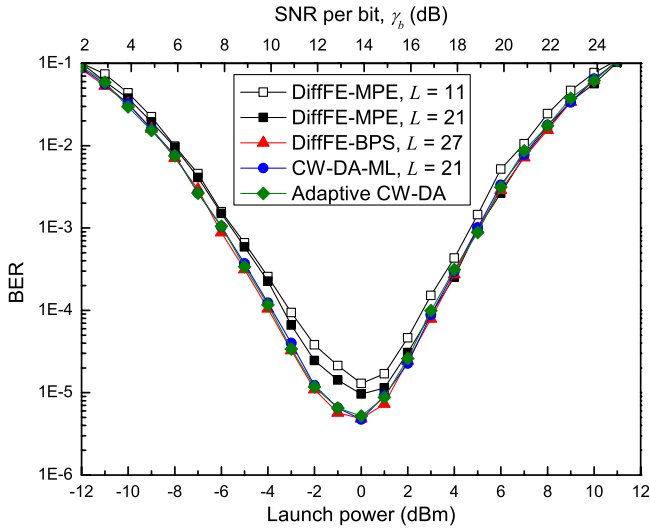


Fig. 8. BER as a function of launch power. Here, $\Delta fT = 0.1$.

IV. PERFORMANCE IN NONLINEAR PHASE NOISE

We consider the presence of fiber Kerr nonlinearity in the optical transmission system illustrated in Fig. 1. Interaction of signal and ASE noise with the Kerr effect generates self-phase-modulation induced nonlinear phase noise [23]. The accumulated nonlinear phase noise experienced by the signal after N_{span} EDFAs is given by [24]

$$\theta_{NL}(k) = \gamma \left(\frac{1 - \exp(-\alpha L_{fiber})}{\alpha} \right) \cdot \left| \sum_{j=1}^{N_{span}} \left[m(k) + \sum_{i=1}^j n_i(k) \right] \right|^2 \quad (8)$$

where γ is the nonlinear coefficient of the fiber. The received sample in (1) is now corrupted by a total phase noise of $\theta(k) = \theta_L(k) + \theta_{NL}(k)$. Nonlinear phase noise impairs the performance of phase-modulated optical systems [25].

Fig. 8 analyzes the nonlinear phase noise tolerance of carrier estimators in a 28-Gbaud QPSK signal transmission over $N_{span} = 41$ spans. A nominal combined laser linewidth of 200 kHz is used and the following system parameters are assumed: $\gamma = 1.2 \text{ W}^{-1} \text{ km}^{-1}$, $L_{fiber} = 100 \text{ km}$, $\alpha = 0.2 \text{ dB/km}$, $G = 20 \text{ dB}$, optical wavelength $\lambda = 1550 \text{ nm}$, $n_{sp} = 1.41$, and $B_0 = 28 \text{ GHz}$. The optimum filter length for DiffFE-MPE, DiffFE-BPS, and CW-DA-ML was found to be 21, 27, and 21, respectively, through an exhaustive search. In contrast, our new estimator automatically adapts its effective filter length according to the nonlinear phase noise to achieve the lower BER. The minimum BER occurs at approximately 0 dBm launch power corresponding to a mean nonlinear phase shift of 1.07 rad [24], which agrees well with the finding of [23]. As the launch power exceeds the optimum power, variance of the total phase noise increases and the BER deteriorates. Adaptive CW-DA estimator approximately halves the minimum achievable BER compared to DiffFE-MPE.

In order to understand the effect of nonlinear phase noise on cycle slip probability, we kept the SNR per bit constant at 4.47 dB in Fig. 8 and varied the launch power. The resulting

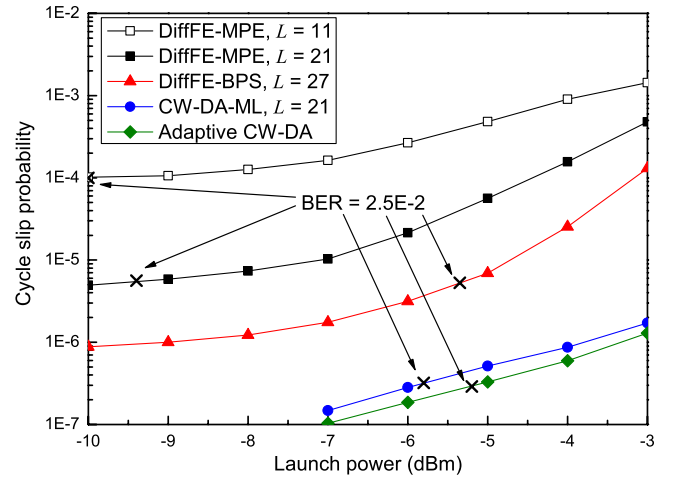


Fig. 9. Cycle slip probability as a function of launch power at $\gamma_b = 4.47 \text{ dB}$.

TABLE I
COORDINATES OF POINTS AT BER OF 2.5×10^{-2} IN FIG. 9

| Carrier estimator | Launch power (dBm) | Cycle slip probability |
|----------------------|--------------------|------------------------|
| DiffFE-MPE, $L = 11$ | -10.0 | 1.0×10^{-4} |
| DiffFE-MPE, $L = 21$ | -9.4 | 5.6×10^{-6} |
| DiffFE-BPS, $L = 27$ | -5.4 | 5.3×10^{-6} |
| CW-DA-ML, $L = 21$ | -5.8 | 3.2×10^{-7} |
| Adaptive CW-DA | -5.2 | 2.9×10^{-7} |

cycle slip probability is plotted in Fig. 9. The value of n_{sp} was varied to keep the SNR constant. The nonlinear phase shift increases with the launch power, thereby increasing the cycle slip probability. A cycle slip probability floor appears for DiffFE-MPE and DiffFE-BPS employing fixed-length filters, similar to the linear phase noise case in Fig. 6. Points yielding a BER of 2.5×10^{-2} with differential encoding are marked in Fig. 9 and tabulated in Table I. The importance of filter-length adjustment is illustrated by DiffFE-MPE using $L = 11$ and $L = 21$. Filter-length adjustment from 11 to 21 yields a minimal 0.6-dB improvement in launch power tolerance at a BER of 2.5×10^{-2} , but successfully avoids a TDD post-FEC error floor of 10^{-9} by reducing the cycle slip probability from 10^{-4} to 5.6×10^{-6} . From Table I, we observe that the adaptive CW-DA estimator achieves greater nonlinear phase noise tolerance and lower cycle slip probability than the other estimators.

V. COMPLEXITY ANALYSIS

Carrier estimators should have a low computational complexity in order to be feasible for practical implementation with data rates of 100 Gb/s and beyond. Thanks to adaptive CW-DA estimator's two-tap filter structure, the computational complexity is greatly simplified. We compute and store only the upper triangle of the matrix Φ in (6) while the lower triangle is obtained by diagonal reflection, as Φ is Hermitian. Summations in (6) and (7) can be computed recursively. Furthermore, the matrix inversion in (5) is trivial as Φ is a 2-by-2 matrix.

Table II analyzes the computational complexity of carrier estimators for QPSK signals. Each complex multiplication is

TABLE II
COMPLEXITY ANALYSIS

| Estimator | Complexity to estimate | Real multiplications | Real additions | Intermediate decisions | Comparisons | Table look-ups | Phase unwrap | Buffer units |
|----------------|---------------------------------|----------------------|----------------|------------------------|-------------|----------------|--------------|--------------|
| DiffFE | $\Delta\omega$ over N symbols | $12(N-1)+1$ | $6(N-1)+2N-2$ | 0 | 0 | 1 | 0 | 0 |
| | | 119989 | 79992 | 0 | 0 | 1 | 0 | 0 |
| MPE | $\theta(k)$ per symbol | $8+1/L$ | $6-2/L$ | 0 | 0 | $1/L$ | $1/L$ | 0 |
| | | 8.07 | 5.87 | 0 | 0 | 0.07 | 0.07 | 0 |
| BPS | $\theta(k)$ per symbol | 6β | $(L+4)\beta$ | β | β | 0 | 1 | $L\beta$ |
| | | 192 | 736 | 32 | 32 | 0 | 1 | 608 |
| CW-DA-ML | $V(k)$ per symbol | $6L^2+14L+10$ | $6L^2+8L+6$ | 0 | 0 | 0 | 0 | L^2+6L+4 |
| | | 1570 | 1476 | 0 | 0 | 0 | 0 | 319 |
| Adaptive CW-DA | $V(k)$ per symbol | 43 | 34 | 0 | 0 | 0 | 0 | 12 |

calculated as four real multiplications and two real additions. Each $\arctan(\cdot)$ operation is expressed as a table lookup. Complexity of DiffFE is presented separately, as DiffFE estimates the frequency over a block of N symbols whereas adaptive CW-DA estimator estimates the phase and frequency on a symbol-by-symbol basis.

Our new estimator does not require any intermediate decisions, comparisons, table look-ups, or phase unwrapping. Adaptive CW-DA estimator has a fixed complexity, unlike MPE and BPS whose complexity varies with L and β . Representative numbers are also given in Table II by substituting practical values for DiffFE ($N = 10^4$), MPE ($L = 15$), BPS ($L = 19, \beta = 32$), and CW-DA-ML ($L = 15$) [10], [17]. Our new estimator reduces the multiplications, additions, and buffer units by a factor of 36.5, 43.4, and 26.6, respectively, compared to CW-DA-ML. Although BPS only estimates the phase, it still needs 4.5, 21.6, and 50.7 times more multiplications, additions, and buffer units, respectively, compared to our new estimator.

Further reduction of our estimator's complexity can be achieved in an application specific integrated circuit (ASIC) implementation, for example, by using the coordinate rotation digital computing technique [26]. We remark that the required digital resolution of the ASIC, in terms of number of bits, to minimize the signal quantization penalty will also affect the implementation complexity.

VI. CONCLUSION

A judicial choice of filter length is crucial in carrier estimators using fixed-length filters such as MPE, BPS, and CW-DA-ML, regardless of their deployment in a pilot assisted or a differentially encoded system. Although the degradation in the required SNR or nonlinear phase noise tolerance is minimal when the filter length is not optimized, the resulting degradation in cycle slip probability can cause system failures.

We presented a low-complexity adaptive CW-DA estimator which automatically adapts its effective filter length according to the SNR, laser-linewidth-symbol-duration product $\Delta\nu T$, nonlinear phase noise, and modulation format. The adaptive CW-DA estimator has similar $\Delta\nu T$ tolerance as MPE and CW-DA-ML, but slightly smaller compared to BPS. However, the

SNR per bit penalty compared to BPS is a mere 0.25 dB at $\Delta\nu T = 4.1 \times 10^{-4}$. Our new estimator achieves a lower or equal cycle slip probability compared to DiffFE-MPE, DiffFE-BPS, and CW-DA-ML, in linear and nonlinear phase noise systems. Additionally, a larger nonlinear phase noise tolerance than the other estimators and a complete frequency estimation range is achieved. To further endeavor adaptive CW-DA estimator to reconfigurable optical networks, the estimator should be parallelized, which is a subject of future work.

REFERENCES

- [1] E. B. Basch, R. Egorov, S. Gringeri, and S. Elby, "Architectural trade-offs for reconfigurable dense wavelength-division multiplexing systems," *IEEE J. Sel. Topics Quantum Electron.*, vol. 12, no. 4, pp. 615–626, Jul./Aug. 2006.
- [2] S. J. B. Yoo, "Optical packet and burst switching technologies for the future photonic internet," *J. Lightw. Technol.*, vol. 24, no. 12, pp. 4468–4492, Dec. 2006.
- [3] O. Gerstel, M. Jinno, A. Lord, and S. J. B. Yoo, "Elastic optical networking: a new dawn for the optical layer?" *IEEE Commun. Mag.*, vol. 50, no. 2, pp. s12–s20, Feb. 2012.
- [4] S. Gringeri, N. Bitar, and T. J. Xia, "Extending software defined network principles to include optical transport," *IEEE Commun. Mag.*, vol. 51, no. 3, pp. 32–40, Mar. 2013.
- [5] K. Roberts and C. Laperle, "Flexible transceivers," in *Proc. ECOC*, Amsterdam, The Netherlands, 2012, paper We.3.A.3.
- [6] W.-R. Peng, I. Morita, and H. Tanaka, "Hybrid QAM transmission techniques for single-carrier ultra-dense WDM systems," in *Proc. OECC*, Kaohsiung, Taiwan, 2011, pp. 824–825.
- [7] Q. Zhuge *et al.*, "Time domain hybrid QAM based rate-adaptive optical transmissions using high speed DACs," in *Proc. OFC/NFOEC*, Anaheim, CA, 2013, paper OTh4E.6.
- [8] F. Vacondio *et al.*, "Coherent receiver enabling data rate adaptive optical packet networks," in *Proc. ECOC*, Geneva, Switzerland, 2011, paper Mo.2.A.4.
- [9] D. S. Ly-Gagnon, S. Tsukamoto, K. Katoh, and K. Kikuchi, "Coherent detection of optical quadrature phase-shift keying signals with carrier phase estimation," *J. Lightw. Technol.*, vol. 24, no. 1, pp. 12–21, Jan. 2006.
- [10] T. Pfau, S. Hoffmann, and R. Noe, "Hardware-efficient coherent digital receiver concept with feedforward carrier recovery for M -QAM constellations," *J. Lightw. Technol.*, vol. 27, no. 8, pp. 989–999, Apr. 2009.
- [11] M. Seimetz, "Laser linewidth limitations for optical systems with high-order modulation employing feed forward digital carrier phase estimation," in *Proc. OFC/NFOEC*, San Diego, CA, 2008, paper OTuM2.
- [12] D. van den Borne *et al.*, "Carrier phase estimation for coherent equalization of 43-Gb/s POLMUX-NRZ-DQPSK transmission with 10.7-Gb/s NRZ neighbours," in *Proc. ECOC*, Berlin, Germany, 2007, paper 7.2.3.

- [13] A. Leven, N. Kaneda, U.-V. Koc, and Y.-K. Chen, "Frequency estimation in intradyne reception," *IEEE Photon. Technol. Lett.*, vol. 19, no. 6, pp. 366–368, Mar. 2007.
- [14] P.-Y. Kam, "Maximum likelihood carrier phase recovery for linear suppressed-carrier digital data modulations," *IEEE Trans. Commun.*, vol. 34, no. 6, pp. 522–527, Jun. 1986.
- [15] P.-Y. Kam, K. H. Chua, and X. Yu, "Adaptive symbol-by-symbol reception of MPSK on the Gaussian channel with unknown carrier phase characteristics," *IEEE Trans. Commun.*, vol. 46, no. 10, pp. 1275–1279, Oct. 1998.
- [16] A. Meiyappan, P.-Y. Kam, and H. Kim, "Performance of decision-aided maximum-likelihood carrier phase estimation with frequency offset," in *Proc. OFC/NFOEC*, Los Angeles, CA, 2012, paper OTu2G.6.
- [17] A. Meiyappan, P.-Y. Kam, and H. Kim, "On decision aided carrier phase and frequency offset estimation in coherent optical receivers," *J. Lightw. Technol.*, vol. 31, no. 13, pp. 2055–2069, Jul. 2013.
- [18] A. Meiyappan, P.-Y. Kam, and H. Kim, "A low-complexity carrier phase and frequency offset estimator with adaptive filter length for coherent receivers," in *Proc. ECOC*, London, U.K., 2013, paper P.3.6.
- [19] *Forward Error Correction for High Bit-Rate DWDM Submarine Systems*, ITU-T Recommendation G.975.1, 2004.
- [20] T. Mizuochi, "Recent progress in forward error correction and its interplay with transmission impairments," *IEEE J. Sel. Topics Quantum Electron.*, vol. 12, no. 4, pp. 544–554, Jul./Aug. 2006.
- [21] F. Yu *et al.*, "Soft-decision LDPC turbo decoding for DQPSK modulation in coherent optical receivers," in *Proc. ECOC*, Geneva, Switzerland, 2011, paper We.10.P11.70.
- [22] A. Bisplinghoff, S. Langenbach, T. Kupfer, and B. Schmauss, "Turbo differential decoding failure for a coherent phase slip channel," in *Proc. ECOC*, Amsterdam, The Netherlands, 2012, paper Mo.1.A.5.
- [23] J. P. Gordon and L. F. Mollenauer, "Phase noise in photonic communications systems using linear amplifiers," *Opt. Lett.*, vol. 15, no. 23, pp. 1351–1353, Dec. 1990.
- [24] K.-P. Ho and J. M. Kahn, "Electronic compensation technique to mitigate nonlinear phase noise," *J. Lightw. Technol.*, vol. 22, no. 3, pp. 779–783, Mar. 2004.
- [25] H. Kim and A. H. Gnauck, "Experimental investigation of the performance limitation of DPSK systems due to nonlinear phase noise," *IEEE Photon. Technol. Lett.*, vol. 15, no. 2, pp. 320–322, Feb. 2003.
- [26] J. E. Volder, "The CORDIC trigonometric computing technique," *IRE Trans. Electron. Comp.*, vol. EC-8, no. 3, pp. 330–334, Sep. 1959.

Adaickalavan Meiyappan (S'13) received the B.E. degree in electrical engineering from the National University of Singapore, Singapore, in 2010, where he is currently working toward the Ph.D. degree in electrical engineering.

His research interest includes digital signal processing for coherent optical communication systems.

Hoon Kim (S'97–A'00–M'04–SM'11) received the M.S. and Ph.D. degrees in electrical engineering from the Korea Advanced Institute of Science and Technology, Taejeon, Korea, in 1996 and 2000, respectively.

From 2001 to 2002, he was with Bell Laboratories, Lucent Technologies, where he worked on advanced optical modulation formats. From 2002 to 2007, he was with Samsung Electronics, Suwon, Korea, where he was involved in research on optical duobinary transmission systems, optical sources for access applications, and fiber-optic networks for wireless communications. Since 2007, he has been an Assistant Professor with the Department of Electrical and Computer Engineering, National University of Singapore.

Dr. Kim now serves as an Associate Editor of *IEEE PHOTONICS TECHNOLOGY LETTERS* and has served on several international conferences as technical committee member, including Optical Fiber Communication, IEEE Lasers Electro-Optics Society, OptoElectronics and Communication Conference, and Asia-Pacific Optical Communications.

Pooi-Yuen Kam (F'10) was born in Ipoh, Malaysia. He received the S.B., S.M., and Ph.D. degrees in electrical engineering from the Massachusetts Institute of Technology, Cambridge, MA, USA, in 1972, 1973, and 1976, respectively.

From 1976 to 1978, he was a member of the technical staff at the Bell Telephone Laboratories, Holmdel, NJ, USA, where he was engaged in packet network studies. Since 1978, he has been with the Department of Electrical and Computer Engineering, National University of Singapore, where he is currently a Professor. He served as the Deputy Dean of Engineering and the Vice Dean for Academic Affairs, Faculty of Engineering of the National University of Singapore, from 2000 to 2003. His research interests include communication sciences and information theory, and their applications to wireless and optical communications. He spent the sabbatical year 1987 to 1988 at the Tokyo Institute of Technology, Tokyo, Japan, under the sponsorship of the Hitachi Scholarship Foundation. In year 2006, he was invited to the School of Engineering Science, Simon Fraser University, Burnaby, B.C., Canada, as the David Bested Fellow.

Dr. Kam is a member of Eta Kappa Nu, Tau Beta Pi, and Sigma Xi. Since September 2011, he is a Senior Editor of the *IEEE WIRELESS COMMUNICATIONS LETTERS*. From 1996 to 2011, he served as the Editor for Modulation and Detection for Wireless Systems of the *IEEE TRANSACTIONS ON COMMUNICATIONS*. He also served on the editorial board of PHYCOM, the *Journal of Physical Communications* of Elsevier, from 2007 to 2012. He was elected a Fellow of the IEEE for his contributions to receiver design and performance analysis for wireless communications. He received the Best Paper Award at the IEEE VTC2004-Fall, at the IEEE VTC2011-Spring, and at the IEEE ICC2011.